American Journal of Science

FEBRUARY 1940

STRUCTURAL PETROLOGY OF THE SCHISTS OF EASTERN OTAGO, NEW ZEALAND.[1]

F. J. TURNER.

Contents.

PART I.

GEOLOGICAL SETTING OF THE PROBLEM.

SCHISTS of low metamorphic rank, usually referred to as the Maniototo or Wanaka series,[2] cover an area of about 600 square miles in the province of Otago, South Island of New Zealand. This "series," which embraces a wide stratigraphic range, includes rocks at least as old as Permian, for there is southward transition with decreasing metamorphism into greywackes and slates of that age (Te Anau and Clinton series). To the north-east late Tertiary faults of great throw separate the Maniototo schists from greywackes and slaty rocks which locally contain mid-Triassic fossils and which have themselves been subjected to deformation involving widespread development of rather imperfect schistosity even in the resistant grey-

[1] Results of work carried out in 1938-1939 as a Sterling Fellow of Yale University.

[2] The schists of Otago Province have been described by various writers as the Wanaka, Maniototo, or Tuapeka series. Various members of the schist group are stratigraphically equivalent to almost unmetamorphosed rocks to which yet other names have been given, e.g. the Te Anau series. The term Kakanui series has been applied to fissile greywackes, slates, and phyllonites that flank the schist belt of Otago on the north-east; these rocks, possibly of mid-Mesozoic age, are outside the scope of the present paper.

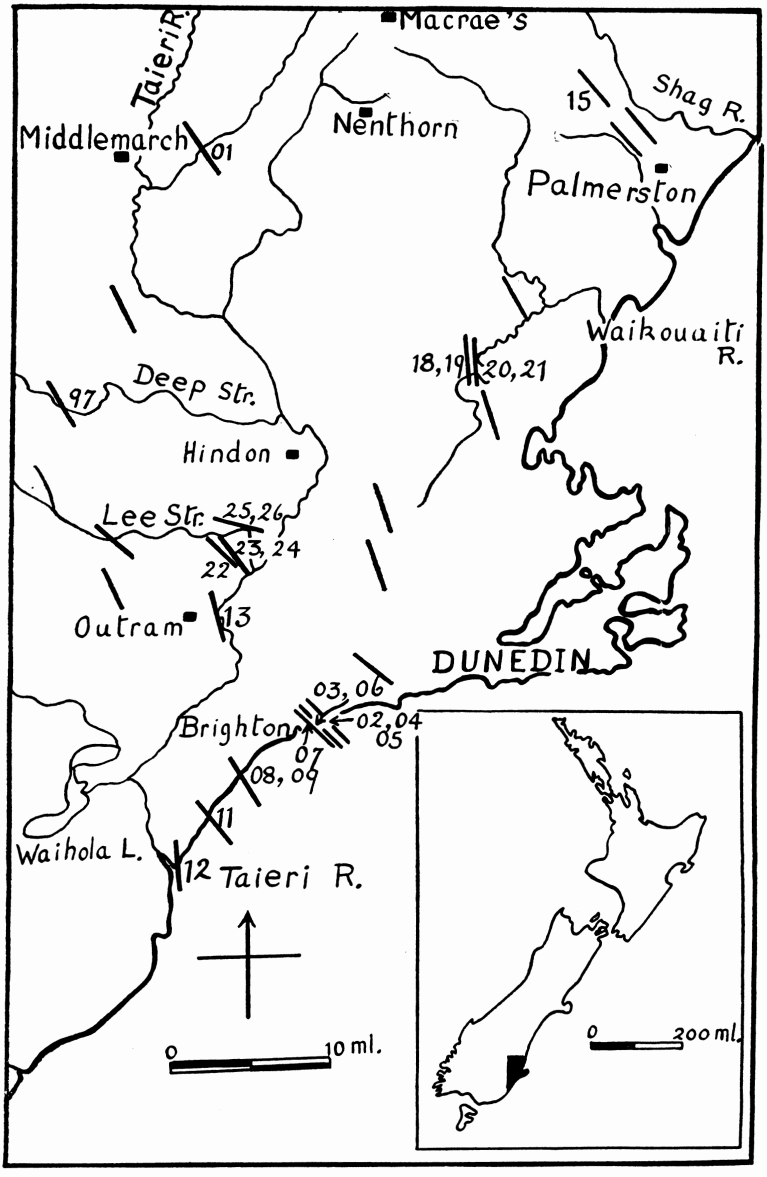

Fig. A. Map of a part of Eastern Otago. Trend of main lineation (b) in schists at representative stations is shown by solid bars. Localities of measured specimens referred to in this paper are indicated by the last two figures of the specimen number. Inset map shows the islands of New Zealand with the area here investigated in solid black.

wacke members (Mackie, 1936). Metamorphism of the schists of Otago is believed by some workers to be a result of deformation during the late Jurassic Hokonui orogeny, which certainly is responsible for the contorted condition of the flanking Triassic and Jurassic rocks, but the writer considers it more likely that the main phase of metamorphism preceded deposition of the mid-Triassic strata.

The main petrographic features of the schists of Otago have recently been summarized in a paper by the writer (Turner, 1938).

The present paper concerns the eastern coastal portion of the schist zone of Otago between the Taieri and Shag rivers. Beyond the southern limit of the map metamorphism gradually decreases and the schistose rocks pass stratigraphically upward into greywackes with Permian fossils (Clinton series), which still farther south are overlain by folded Triassic and Jurassic strata, while to the north they have been brought into juxtaposition with folded, non-fossiliferous, possibly Triassic greywackes by repeated movements of great magnitude along the Shag Valley fault-zone. Following the Hokonui folding, schists and greywackes alike were eroded to a peneplain upon which marine sediments ranging from late Cretaceous to late Oligocene in age were subsequently deposited. Regional uplift, followed by further extensive erosion took place in the later part of the Tertiary, while large-scale Pliocene block-faulting is responsible for the present relief of about 4,000 feet, and the gently tilted condition of the sedimentary cover and the partially stripped lower Cretaceous peneplain surface. The youngest rocks in eastern Otago are the Pliocene lavas of the Dunedin volcanic complex, which also have been affected by movements continuing into recent times.

Petrographically the schists of the east coast belt are for the most part rather coarse-grained quartzo-feldspathic types, the principal constituents of which are albite, quartz, muscovite, chlorite, and an epidote mineral, sometimes with plentiful stilpnomelane in addition. Constant accessories are apatite, tourmaline, zircon, and finely divided iron-ore; opaque, dusty material freely developed along obvious surfaces of slip in the more strongly deformed rocks may possibly be either iron oxides or graphite but has not been determined with certainty. Small amounts of calcite and garnet occur in some rocks, while in coarsely porphyroblastic albite-schists from one locality

(Nos. 4718,[3] 4721) a greenish-brown micaceous mineral probably biotite, but perhaps a member of the stilpnomelane group, is abundant.

Oriented specimens of typical rocks have been collected from fifteen stations within the area under consideration, and details of megascopic structure (schistosities, lineations, joints, veins) have been recorded at these as well as other localities.[4] Oriented sections have been cut and subjected to petrofabric analysis by the standard universal-stage methods of investigation developed by Sander and Walter Schmidt. From the appearance of polished specimens alone it is clear that the structure of the schists is highly complex. Therefore in order to evaluate the regional significance of the facts brought out by fabric analysis, the following procedure has been applied as far as time would permit. First the fabric elements are measured and compared for separate limited areas within a single rock-section; then for different sections of the same rock or for sections cut from specimens taken within a few feet from the same outcrop; then for sections representing materials from adjacent localities, and finally for specimens from widely separated stations. In this way regionally and locally significant features may be distinguished and the degree to which a regionally important feature is subject to variation is brought out.

SUMMARY OF RESULTS.

The results of an investigation of this type are the facts recorded in the fabric diagrams. Therefore these are given as fully as possible, together with appropriate field data and explanatory notes, in the later part of the paper. In order that these recorded data may be understood more readily, the writer's general interpretation of their tectonic significance is first presented in condensed form, the reader being referred to particular instances for the evidence on which the conclusions are based.

Before enumerating these results, however, attention is drawn to the necessity for determining to what extent the preferred orientation of the minerals investigated is related to the features of the megascopic fabric. It will be found for example

[3] Numbers refer to specimens and corresponding sections in the collections of the Department of Geology, University of Otago, Dunedin, New Zealand.

[4] For localization of specimens, see map (Fig. A).

that the mica and chlorite patterns are strongly influenced by the schistosity, while the quartz pattern, on the other hand, is almost unrelated. It is therefore necessary to establish the relative order of the two phases of metamorphism involving the imprints of the chlorite-mica fabric and the quartz fabric respectively.

(1) Over great areas the megascopic schistosity is horizontal or gently inclined, as noted by all previous observers in this field, but locally it dips steeply, often about a NW to NNW strike, while along the coastal section just south of Brighton, the schistosity lies in closely-spaced open folds with a NNW trend. In the northern part of the area, which has been mapped by Service (1933), a north-easterly strike prevails and the dip is uniformly southeast at 12°-30°. The schistosity in the schists of Otago is believed to have developed parallel to the principal surfaces of slip during deformation (cf. Turner, 1936). Distinct evidence of this may be seen in many rocks (e.g. No. 4715) in which alternating quartzose and micaceous laminae have been complexly overfolded on a microscopic scale, and the resultant complex structure cut by low-angle surfaces of slip which now control the schistosity. Where, as in Nos. 4723, 4724, rupture of the microfolds has not proceeded far, the schistosity is correspondingly imperfect. Where, as in Nos. 4702-4707 from immediately north of Brighton, more than one schistosity is conspicuous, local rapid variation in their relative degree of development confuses field measurements of dip.

(2) A strong lineation, tentatively selected as the *b* fabric axis, is always present in the plane of schistosity and trends between NW and 5°-10° W of N, as shown on the map (Fig. A). In rocks with conspicuous microfolds the lineation *b* (B) is the axis of folding, while in other rocks *b* is either parallel to minute corrugations developed in the micaceous layers or is the line of intersection of several schistosities (e.g. Nos. 4702-4706). In all cases it appears to be the B-axis connected with the earliest and main phase of metamorphism. A second lineation *b′*, striking NNW to N and always somewhat more northerly than the corresponding *b* of the same rock, is frequently present, especially where the specimen has been broken along a micaceous layer. It has not been found possible definitely to correlate *b′* with any secondary slip surface intersecting the main schistosity, and on this account it is suggested that *b′* repre-

sents a late puckering of micaceous layers by slip in the schistosity plane in a direction transverse to *b′*. A third lineation of local significance is rarely observable and in no case prominently defined (see descriptions of Nos. 4718, 4726).

(3) Segregation of minerals into alternating micaceous and quartz-albite layers is typical, except in schists (e.g. No. 4711) from the southern end of the coastal section where metamorphism attained a lower rank than elsewhere. The vein-like layers of quartz and albite, usually 1 mm. to 5 mm. in thickness, lie parallel to the main schistosity or sometimes to surfaces intersecting in *b* (e.g. No. 4713), or in many instances have been affected by intricate small-scale folding and even complete disruption (e.g. No. 4715). They are considered to be a product of segregation (metamorphic differentiation) during reconstitution accompanying the main phase of metamorphism, for not only do they conform structurally to *b* (the main axis of deformation), but they contain minor constituent minerals such as muscovite, chlorite, stilpnomelane, and apatite which also occur in adjacent non-quartzose layers.

(4) Steeply dipping (often vertical) joints are conspicuous and with the subhorizontal schistosity are responsible for the rectangular, blocky outcrops that are so characteristic of the schist areas of Otago (cf. Finlayson, 1908, pp. 72, 73). The strike of the dominant set of joints varies between NE and E, and in any specific locality is perpendicular to *b′* rather than to *b*. Widely spaced but persistent vertical joints trending NW parallel to the lineation *b* may sometimes be observed where continuous outcrops are exposed, as along the east coastal section. Less conspicuous sets of joints of obscure tectonic significance occur locally. In some localities, e.g. seven miles south of Brighton, quartz veins fill many of the joints, but the vein material has not yet been investigated.

(5) The muscovite, chlorite, and stilpnomelane fabrics as determined by plotting the poles of the (001) cleavage conform to the same general pattern, though usually showing slight differences in any given rock. The dominant feature is a well-defined girdle with prominent maxima corresponding to directions of slip visible in the section, and submaxima of other significance to be discussed below. Since the schistosity surfaces in many rocks are not exactly planar, the mica maximum of any given diagram often does not exactly coincide with the mean pole of the schistosity as determined from the hand-speci-

men. The girdles for these three micaceous minerals, though almost centred about *b*, are consistently displaced by small amounts so that the centre of the girdle lies between *b* and *b′* (e.g. Figs. 25-30, 32, 37, 38). Though slight, this eccentricity is certainly significant, for it is always shown by diagrams for both mica and chlorite in any one rock, and is always in the same direction.[5] The writer believes that the mica fabric, originally developed concentrically about *b* during the first stages of metamorphism, has later been partially reoriented by movement across the axis *b′*. This movement has also been sufficiently intense to initiate a secondary lineation in some layers though not intense enough to bring the whole fabric into conformity with *b′*.

(6) Individual flakes of mica, chlorite, and stilpnomelane, whether constituents of the undulating micaceous layers or scattered crystals enclosed in the quartzo-feldspathic areas, are almost always sharply crystallized and undeformed. Crystallization of these minerals is therefore post-tectonic in relation to the deformations just discussed, and has proceeded either from oriented seed-crystals, or simply in the surfaces and directions of maximum ease of growth. The notable extent to which slip-surfaces, developed at all stages of deformation, are preserved in the mica and chlorite fabrics favour the first of these alternative processes as having had the greater influence.

(7) The quartz fabric as determined by plotting poles of optic axes is complex and variable; nevertheless certain constant features emerge when rocks from widely separated localities are compared:

(a) A well defined girdle is centred about an axis that trends approximately NW, and hence usually is eccentric with regard to *b* but in the opposite sense to the eccentricity of the mica and chlorite girdles. How far this orientation of the axis of the quartz girdle is a regional feature could be determined only if yet other specimens were investigated; for among the data so far gathered there are several exceptions to the general rule, notably in the case of two adjacent rocks (Nos. 4718 and 4721) in each of which the axis of the quartz girdle trends a few degrees E of N.

[5] That lack of sensitivity in the method of measurement is not responsible for the eccentricity of these girdles is clearly indicated by measuring flakes in a section cut not quite perpendicularly, say 80° or 85° to *b*; the obliquity is readily recognisable in the eccentric girdle of the resulting diagram (e.g. Plate III, Figs. 14, 15, Plate IV, Figs. 24, 25).

(b) In all the diagrams the maxima tend to lie on or close to the periphery of the girdle. Types where the maxima lie on a small circle of the projection (cf. Sander, 1930, D. 19, 52; Fairbairn, 1939, Figs. 5-9), are not represented, though in a few diagrams there is a suggestion of approach to this condition.

(c) On the whole the principal maxima tend to lie within a relatively small angular distance of the pole of the horizontal plane. In other words the optic axes of the quartz grains tend to be concentrated at high inclinations to the geographic horizontal. On the other hand submaxima representing quartz axes in an approximately horizontal position are present in many diagrams (e.g. Plate IV, Figs 21, 23, Plate V, Fig. 31, Plate IX, Fig. 52 etc.).

(d) In many diagrams there is no obvious relation between the quartz maxima and the main *s*-planes indicated by the principal maxima for mica and chlorite, except insofar as is recorded below under (f). This holds good whether the preferred orientation of the quartz is assumed to be controlled by prismatic, rhombohedral, or basal rules.

(e) In rare cases where the quartzose layers or "veins" are cut by slip-surfaces visible in the thin section, the maximum in the corresponding quartz diagram corresponds closely with the trace of the slip-surface in question (e.g. see Plate VII, Fig. 40, specimen No. 4709).

(f) In many diagrams for quartz the maxima correspond exactly to points at 90° to submaxima on the mica and chlorite diagrams (e.g., compare Plate V, Fig. 31 and Plate VI, Fig. 34; Plate III, Figs. 16 and 18). This applies particularly where it has been possible to prepare diagrams representing undeformed mica or chlorite occurring in nests between slip-surfaces visible in thin sections, or in isolated flakes enclosed in the quartzose layers.

(g) The maxima in several of the quartz diagrams are grouped so as to resemble ring maxima such as have been taken by other writers to indicate gliding of quartz grains on rhombohedral planes. In such cases (e.g., Plate V, Fig. 31, Plate VIII, Fig. 49) there is usually no relation between the observed slip-surfaces visible in thin section or the principal slip-surfaces deduced from the mica diagrams, and the *s*-surface that would necessarily be deduced on the hypothesis of rhombohedral gliding in the quartz. The resemblance to ring maxima is therefore probably in many though not necessarily in all cases fortuitous.

The writer's interpretation of these facts is that the quartz fabric and the main features of the mica-chlorite-stilpnomelane fabric have developed independently during two different phases of deformation; that the submaxima of the mica, chlorite, and stilpnomelane diagrams correspond to the same phase of deformation as that responsible for orientation of quartz; and that whether by gliding or by dimensional orientation of acicular fractured seed crystals (cf. Griggs and Bell, 1938), the quartz has tended to assume a preferred orientation mainly with the optic axis in the direction of slip.[6] On this latter assumption the deformation in which the quartz fabric was imprinted involved slip movements predominantly but not entirely in surfaces steeply inclined to the horizontal plane [cf. (c) above]. Such movements would originate by more or less horizontally directed compression as if the rock were being compressed between the jaws of a vise.

(8) From comparison of the fabric diagrams the writer concludes that the quartz fabric has been imprinted subsequently to the development of the present fabric of the micaceous minerals. The main evidence bearing upon this question can be summarized thus:

(a) In rocks from the east coast section three miles south of Brighton (Nos. 4708, 4709) large-scale folding has thrown the schistosity surfaces into anticlines and synclines with a crest-to-crest distance of 20 ft. to 50 ft. The mica fabric conforms to the local trend of the schistosity, but the quartz fabric appears to remain approximately homogeneous throughout the field of a complete fold.

(b) In numerous cases where alternating micaceous and quartzose layers have been contorted and ruptured on a microscopic scale, the micas and chlorites tend to lie parallel to the local direction of banding or of visible *s*-surfaces in any particular part of the thin section, but the quartz fabric is broadly homogeneous throughout the field of the section. Thus the quartz fabric in contorted layers of this type is not capable of being "unrolled" (contrast with Sander, 1930, p. 257) as would be possible if it predated the micro-crumpling. It is difficult to visualize survival of a relatively homogeneous quartz fabric through deformation of such intensity and involving displacements of the order indicated in these rocks.

(c) When some of the mica or chlorite has crystallized late in nests which lie between slip surfaces visible in the thin section and are undisturbed by the movements along these surfaces, correspondence between fabrics for quartz and late mica (or chlorite) is distinct in contrast with the lack of similarity when the preferred orientations of quartz and early mica are compared.

(d) In rocks such as Nos. 4713, 4715 for which many partial

[6] If the "ring maxima" mentioned under (g) should actually represent rhombohedral gliding of quartz, this conclusion would have to be modified, but the lack of accordance between quartz and mica-chlorite fabrics would still remain.

diagrams have been constructed, the data so gained are explicable only if it is assumed that in the main the imprint of the quartz fabric was later than that of the mica-chlorite fabric.

(9) Control of preferred orientation of mineral grains by crystallographic glide-directions rather than by glide-planes alone (cf. Schmidt, 1932, p. 174) is perhaps the explanation for the non-coincidence of girdle axes for quartz and mica or chlorite diagrams.

In Fig. 1A let P be the pole of (001) in a mica flake lying in an *s*-surface SS parallel to the axis *b* of the mica girdle; and let *p* be the pole of the crystallographic glide-direction within (001). If slipping is now initiated in a new *s*-surface S′S′ (parallel to *b*′ the axis of the quartz girdle), the mica flake could rotate about *b* so as to bring P to P″ by way of P′ and *p* to *p*′ and ultimately to *p*″. In

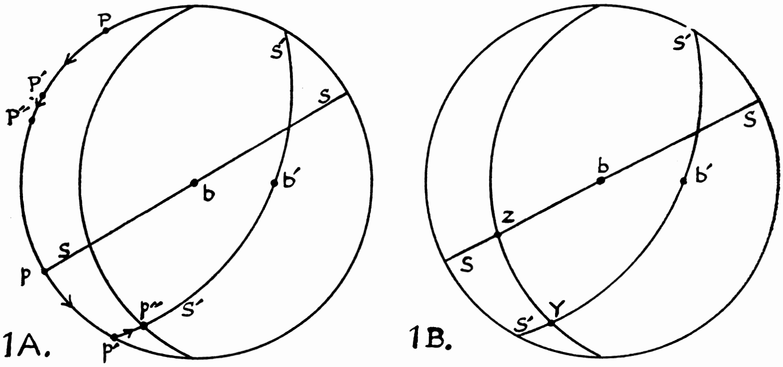

Figs. 1 A, and 1 B. Diagrams illustrating influence of glide-directions on development of preferred orientation in: Fig. 1 A, mica; Fig. 1 B, quartz.

this position, though the pole P″ still lies on the *b* girdle, the flake may now glide along *p*″ at right angles to the new axis *b*′; moreover a mica maximum corresponding to P″ will lie in complementary position to a quartz maximum on the *b*′ girdle representing a concentration of quartz axes parallel to S′S′ and perpendicular to *b*′.

Similarly in Fig. 1B we may picture the quartz fabric as dominated by grains with axes concentrated around Y lying in newly developed *s*-surfaces S′S′, and others with axes at Z lying in earlier planes SS of the *b* series. In both types, however, the quartz axes are oriented perpendicularly to the new direction *b*′.

(10) Where the megascopic schistosity dips steeply, three cases may be distinguished:

(a) Development of a steeply inclined *s*-surface has preceded imprint of the quartz fabric, which therefore conforms to the normal pattern when the geographic horizontal (not the trace of the schistosity) is taken as datum in plotting (e.g. Nos. 4697, 4708, 4709). In such cases the strike of the schistosity is parallel to the lineation *b*, so that it has probably developed as an initially steeply inclined surface during the earliest stage of deformation.

(b) Imprint of the quartz fabric preceded tilting of an initially subhorizontal schistosity, so that the quartz and mica fabrics have been bodily tilted without other modification. Possibly this is a widespread feature in the northeastern part of the area, where NE strikes and SE dips of 12°-30° prevail, but more rocks will have to be investigated to confirm or disprove this.

(c) In zones of intense local faulting the quartz fabric may be almost completely obliterated and a new fabric substituted, the mica remaining unaffected. The single case investigated (No. 4726) is a fault-zone where locally vertical schists have been bevelled by and therefore antedate the Lower Cretaceous peneplain.

THE FABRIC DIAGRAMS.

Explanatory Notes.

In accordance with current practice all diagrams are equal-area projections of the lower hemisphere of reference.

The reference axes *a b* and *c* are chosen with regard to the megascopic fabric: the principal lineation is selected as *b*, and the best defined megascopic schistosity, when present, as the *ab* plane. In all cases investigated, *b* proves to be a B axis by virtue either of rotation of a single set of *s*-surfaces about *b* or of intersection of several sets in *b*. In rocks where the structure is complex the direction of transport (*a* axis), the plane of deformation *ac* (and hence *b*), and the plane *ab* itself may each have occupied different positions at successive stages of a complex deformation. The *a* direction of the earlier stages when the mica fabric was developed may even become the *c* axis of the later stages of deformation during which the quartz fabric was imprinted. To avoid confusion and to facilitate comparison of diagrams prepared for different minerals in the one rock, the *a b* and *c* axes shown on all fabric diagrams are those of the megascopic fabric selected as described above. The SW end of *a*, the SE end of *b* and the upper end of *c* are taken as positive.

For uniformity all diagrams are plotted as for sections cut from the negative (NW) end of *b* and viewed from the NW so that the positive pole of *b* lies at the centre of the projection. Where a section has actually been cut from the positive end of *b* the corresponding diagrams have been replotted by rotating the original through 180° about the horizontal diameter; where this has been necessary the fact is noted in the caption of the figure in question.

When necessary, the trend of visible *s*-surfaces within the area in which measurements were made is indicated diagrammatically by an inset sketch.

Quartz diagrams show the distribution of the optic axes; mica, chlorite and stilpnomelane diagrams show poles of the (001) cleavage.

In most diagrams the horizontal diameter is the trace of the megascopic *ab* plane. Some, however, are plotted with the trace of the geographic horizon as horizontal diameter, the north-east end of which is then indicated by the letters *ne*.

Subhorizontal Schists Between Outram and Mt. Hyde.

North of Outram along the road leading from the Taieri River to Hindon, almost horizontal schists are exposed at intervals for several miles. The simple large-scale structure and completely metamorphosed condition of these rocks (corresponding to Subzone Chl. 4 of the Chlorite Zone) render this a suitable type area. Five representative rocks (Nos. 4713, 4722, 4722a, 4723, 4724) have been examined.

Specimen No. 4724

Locality: Outram-Hindon road, 150 yds. N of second bridge, three miles N of Outram.
Schistosity rather imperfect, dipping SE at 5° to 10°.
Lineations: *b* strong, strike 145°;
b′ faintly developed in micaceous bands, strike 165°-170°.
Joints subvertical, strike 70°, less frequently 15°.

A polished surface cut perpendicularly to *b* shows small-scale crumpling of alternating micaceous and quartzose layers about *b* as fold-axis, the megascopic schistosity being in the main due to subhorizontal orientation of the limbs of ruptured folds.

Rather coarse-grained faintly undulose quartz is associated with albite and sparsely scattered flakes of muscovite and chlorite in the light-coloured layers. In two sections cut at right angles to *b*, a total of 350 quartz grains were measured from four distinct areas of different visible micro-structure. Partial diagrams (three of which are shown as Plate I, Figs. 3, 4, 5) for these different areas are closely similar, especially considering the small number of grains per diagram, so that the quartz fabric is approximately homogeneous for the field of the sections concerned. This is also brought out by comparison with the collective diagram Fig. 2, which represents the total quartz measured. Typical features to which attention is drawn are the slightly eccentric girdle, the maxima grouped on either side of *c*, and faintly indicated submaxima adjacent to *a*.

Muscovite occurs in sharply crystallized undeformed flakelets concentrated in curving streaks and bands. Cursory examination would suggest a low degree of preferred orientation for the mica, for over a limited sector of any micaceous layer the component crystals depart considerably from parallelism with the local trend of the layer in question. Plate I, Fig. 6 depicts the orientation of 300 flakes representative of parts of two thin sections. It shows a definite girdle, almost, but not exactly, concentric as to *b*, with a maximum indicating strong concentration of flakes parallel to the megascopic schistosity *ab*. Doubtless the girdle pattern is in part due to inhomogeneity of the mica fabric arising from the contorted condition of the micaceous layers, so that *b* would be a B-axis of external rotation. But the submaxima at D and E correspond exactly with the maxima similarly lettered on the quartz diagram, Plate I, Fig. 2[7] while there is also approximate coincidence in the case of submaxima F. This is interpreted as indicating alinement of favourably situated micas along the late slip-surfaces that controlled development of the present quartz fabric.

The chlorite diagram (Plate I, Fig. 7) represents 150 relatively coarse undeformed flakes concentrated in chloritic patches or from aggregates bordering the micaceous bands; less numerous crystals enclosed within these latter were excluded so that any influence of mica orientation might be eliminated. As is usually the case in schists from eastern Otago, the crystals of chlorite are noticeably thicker across (001) than are those of mica, and much of the chlorite gives the

[7] Corresponding maxima in diagrams for quartz and mica are situated at 90° to each other.

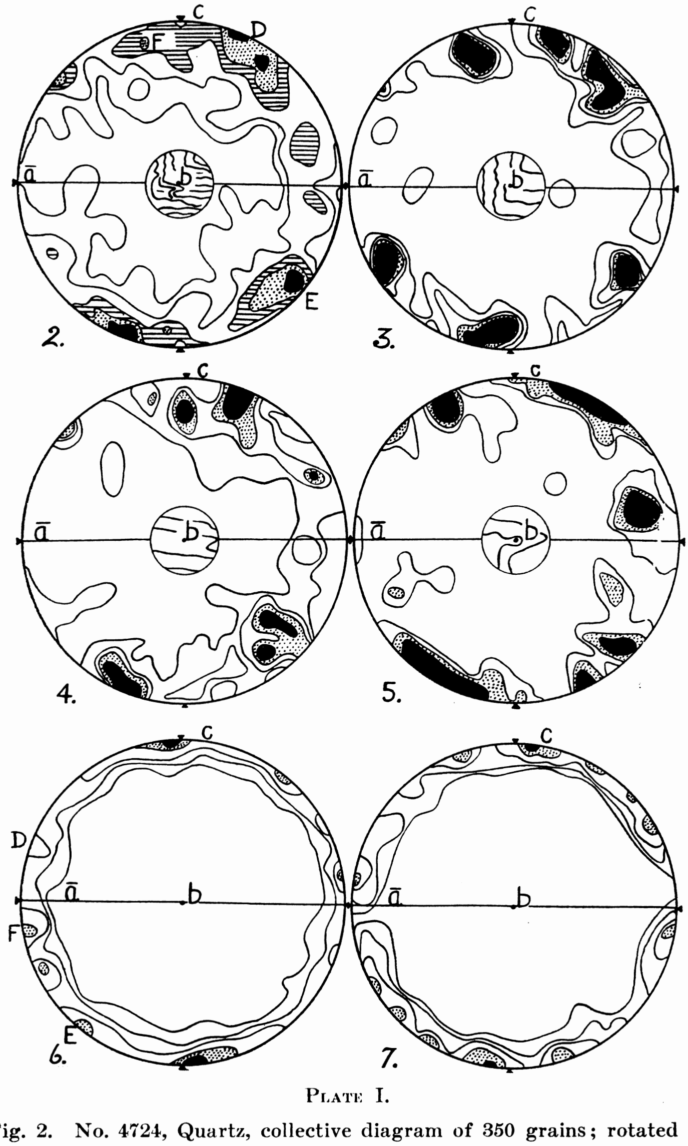

PLATE I.

Fig. 2. No. 4724, Quartz, collective diagram of 350 grains; rotated 180° about *a*. Contours at 4, 3, 2, 1, 0.3%; maximum concentration, 5%.

Fig. 3. No. 4724, Quartz, partial diagram of 82 grains; rotated 180° about *a*. Contours at 4, 3, 2, 1%; maximum concentration, 7%.

Fig. 4. No. 4724, Quartz, partial diagram of 120 grains; rotated 180° about *a*. Contours at 4, 3, 2, 1%; maximum concentration, 6%.

Fig. 5. No. 4724, Quartz, partial diagram of 72 grains in folded area of clear quartz without albite; rotated 180° about *a*. Contours at 4, 3, 1%; maximum concentration, 8%.

Fig. 6. No. 4724, Muscovite, collective diagram of 300 flakes in micaceous layers; rotated 180° about *a*. Contours at 8, 6, 4, 2, 0.3%.

Fig. 7. No. 4724, Chlorite, collective diagram of 150 flakes; rotated 180° about *a*. Contours at 8, 6, 4, 2, 0.7%.

impression of relatively late crystallization. At least segregation of the minute chloritic patches was subsequent to that phase of deformation in which the micaceous bands assumed their present contorted condition. The chlorite and mica diagrams are essentially similar; the maxima almost coincide but there is more divergence as regards submaxima, while the minimum adjacent to *a* is more strongly marked for chlorite than for mica.

Specimen No. 4723.

Locality and megascopic structure the same as recorded for No. 4724. The two specimens were collected two yards apart from the same outcrop. Details of small-scale folding, however, are strikingly different both in the hand-specimen as a whole and in the field of the thin sections (contrast insets in Plate I, Fig. 2 and Plate II, Fig. 8).

Plate II, Fig. 10 is based upon measurements of 300 grains of quartz, many of them coarse and undulose, in a section cut at right angles to *b*, while Plate II, Fig. 11 is a rotated diagram representing 250 grains measured in a section parallel to *ab*. There is a general correspondence between the two, but inexact coincidence of maxima indicates lack of perfect homogeneity of the fabric, though also due in part to influence of superindividuals and to the fewness of the quartz pencils cut by the *ab* as compared with the *ac* section.[8] The characteristic eccentricity of the girdle is more obvious in Plate II, Fig. 11 than in Plate II, Fig. 10. General homogeneity of the quartz fabric is, on the other hand, conclusively indicated when the diagrams for the two rocks (especially Plate I, Fig. 2 and Plate II,

[8] When a large grain recrystallises during deformation as an aggregate of smaller grains, these latter, which are collectively termed a "superindividual" (Sander, 1930, pp. 133, 135), usually show strong preferred orientation which may not be closely related to the preferred orientation exhibited in the fabric as a whole. The influence of superindividuals on the fabric diagrams is minimised by measuring a large number of grains. Experience has shown that in the schists of Otago it is necessary to measure at least 350-400 grains in sections perpendicular to *b* in order to construct a diagram truly representing the quartz fabric of rock. An even greater number of measurements would be required in the case of sections parallel to *b*; for the fabric elements (grains, superindividuals and pencils of quartz) are all elongated parallel to *b* and an *ab* or a *bc* section is therefore less representative of the fabric as a whole than is a section cut perpendicularly to *b*. It follows therefore that Plate II, Fig. 10 (quartz in *ac* section) gives a more complete picture of the quartz fabric than Plate II, Fig. 11 (quartz in *ab* section) in the case under consideration.

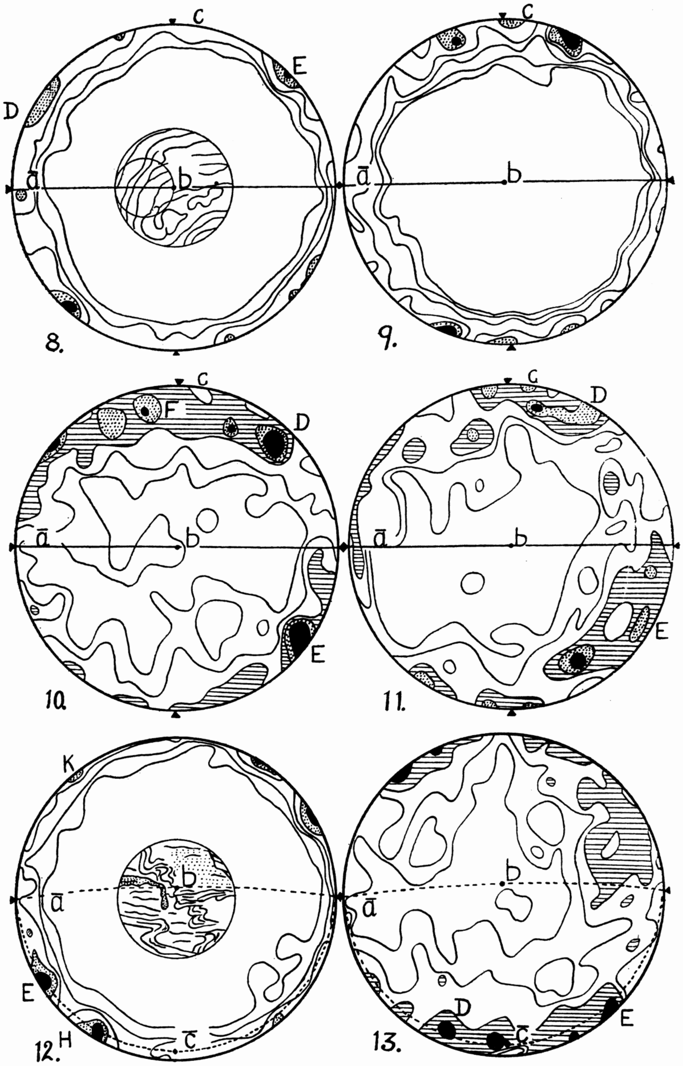

PLATE II.

Fig. 8. No. 4723, Muscovite, 200 flakes in quartz-albite layers; rotated 180° about *a*. Contours at 8, 6, 4, 2, 0.5%. Trend of banding within the measured section is indicated in the smaller inset circle.

Fig. 9. No. 4723, Chlorite, 250 small flakes in quartz-albite layers; rotated 180° about *a*. Contours at 8, 6, 4, 2, 0.4%; maximum concentration 10%.

Fig. 10. No. 4723, Quartz, 300 grains; rotated 180° about *a*. Contours at 4, 3, 2, 1, 0.3%; maximum concentration, 5%.

Fig. 11. No. 4723, Quartz, 250 grains measured in *ab* section; diagram rotated 90° about *a*. Contours at 4, 3, 2, 1, 0.4%.

Fig. 12. No. 4722a, Muscovite, 200 flakes in albitic and quartzose portions of a limited field corresponding to middle left part of inset. Contours 8, 6, 4, 2, 0.5%. Diameter of inset, 20 mm.

Fig. 13. No. 4722a, Quartz, 320 grains in quartz-rich layers (stippled in inset of Fig. 12). Contours 3, 2, 1, 0.3%; maximum concentration, 3.5%.

Fig. 10) are compared, and this constitutes good evidence for late imprint of the preferred orientation now shown by quartz in these rocks.

Since the *ac* section was cut from a quartz-rich part of the rock, measurement of mica was restricted to small isolated flakes and rare nests of coarser crystals enclosed within the quartzo-feldspathic areas. The resultant diagram (Plate II, Fig. 8) shows a well developed, slightly eccentric girdle with strong maxima D and E corresponding exactly with quartz maxima of Plate II, Fig. 10. Concentration of poles at D is probably due at least in part to the local trend of the visible *s*-surfaces (shown in the smaller inset circle), and this is borne out by greater total concentration in the top left than in the top right quadrant, but no such explanation is possible for the maximum E. As in the case of No. 4724, it seems logical to deduce late slip movements upon a double set of surfaces, which are not only responsible for imprinting the quartz fabric but have also influenced the orientation of mica to a notable extent.

The 250 flakes of chlorite upon which Plate II, Fig. 9 is based were also taken entirely from the quartzose portions of the rock. The diagram differs considerably from Plate II, Fig. 8 as a result mainly of the greater tendency for the chlorite to lie subparallel to the schistosity-plane *ab*, and more closely resembles the chlorite diagram (Plate I, Fig. 7) for No. 4724.

Specimen No. 4722a

Locality: Outram-Hindon Road, first bridge, two and one-half miles N of Outram.
Schistosity (*ab*) distinct, dipping SE at 10°.
Lineations: *b* strong, strike 135°;
b′ distinct, strike 155° to 160°.
Joints vertical, regular, strike 75°.
Thin section cut at 84° to *b*.

On the polished end of a specimen cut normal to *b*, steeply dipping, intricately folded light and dark bands are cut by the schistosity which is more or less parallel to the axial planes of the corrugations. In thin section the micaceous bands are seen to have ruptured along surfaces of slip (*ab*) outlined in black dusty material, while in the quartzose and albitic layers, strings of mica are also developed subparallel to *ab* (cf. inset, Plate II, Fig. 12).

A total of 320 grains of quartz, taken mainly from two bands containing relatively little albite and mica, are represented in Plate II, Fig. 13, which shows the usual concentration of maxima on either side of *c* and the characteristic girdle notably eccentric with reference to *b*. Similarity to Plate I, Fig. 2 is specially marked.

The flakes of mica are small, clear-cut, and undeformed. The diagram (Plate II, Fig. 12) is based upon 200 isolated flakes from albitic and to a less extent from quartzose layers. To ascertain any relation between preferred orientation of the mica and the trend of the banding, measurement was confined to crystals lying in a restricted field (middle left portion of inset, Plate II, Fig. 12), in which locally the visible *s*-surfaces intersect *ab* at angles of less than 40°. Two principal maxima are developed, of which one (E) corresponds with the quartz maximum similarly lettered, while the second shows the influence of the *s*-surfaces visible in the measured sector.

In the same field of measurement, only 60 flakes of chlorite were available. Though insufficient to warrant construction of a diagram, they indicate a decided tendency for concentration of the poles towards the middle of the periphery of the bottom left quadrant in much the same way as recorded above for mica.

Specimen No. 4722.

Locality, schistosity, lineations and joints, are all as for No. 4722a. The two specimens were collected three feet apart from the same continuous outcrop. A polished specimen cut perpendicularly to *b* shows much more complete and regular development of the schistosity (*ab*), with complementary elimination of the contorted structure observed in the adjacent rock. Undulating vein-like layers rich in quartz lie parallel to *b* and cut the schistosity (*ab*) at angles of less than 25°.

The thin section in which quartz, mica, and stilpnomelane were measured was by mistake cut eccentrically at an angle of 78° to *b* as indicated in the accompanying fabric diagrams.

Grains of quartz were measured in the two largest of the stippled areas of Plate III, Fig. 14 (inset diagram) and the results first plotted as separate partial diagrams, which on account of their general similarity were then combined into the single collective diagram, Plate III, Fig. 16, based on 330 grains in all. This shows the same general features as Plate II, Fig. 13 (No. 4722a), but the central minimum around *b* is less clearly marked and there is a definite tendency for the maxima D and E to be drawn out towards *b*. Plate III, Fig. 17 shows the result of measurement of 250 grains of quartz in a *bc* section,[9] with subsequent rotation through 90° into the *ac* position. Comparison of the two diagrams suggests that within the field of the hand-specimen the quartz fabric is not perfectly homogeneous. This is also brought out by slight differences in partial diagrams for the same quartz-rich layer as measured in sections parallel respectively to *ac* and to *bc*. From Plate II, Fig. 13, Plate III, Figs. 16 and 17, it is therefore concluded that for the rocks of this locality the quartz fabric conforms to a broadly constant pattern, but nevertheless has not attained a condition of perfect homogeneity even within the field of a small hand-specimen.

Undeformed crystals of muscovite occur abundantly in the mica-albite layers, both as isolated flakes scattered through a matrix of albite, and as the main constituents of discontinuous, narrow, undulating, micaceous streaks. Measurements were confined to an area corresponding to the lower left quadrant of the inset circle in Plate III, Fig. 14, where three traverses across the schistosity were made involving 300 flakes in all. The three resultant partial diagrams proved to be almost identical and were therefore combined into the collective diagram, Plate III, Fig. 14. A second mica diagram (Plate III, Fig. 15) represents the preferred orientation of 200 isolated flakes of muscovite enclosed in the quartzose layers, while Plate III, Fig. 18 is based upon 150 undeformed crystals of deep brown stilpnomelane in the quartz band shown in the lower half of the inset circle in Plate III, Fig. 14. These three diagrams and Plate II, Fig. 12 are closely similar and the maxima have therefore been lettered to correspond in all four. The main concentration of poles in Plate III, Fig. 14 is close to *c* as would be expected from the abundance of micaceous streaks lying more or less parallel to *a* in the area investigated, but in the quartzose bands where such streaks are lacking the influence of the main schistosity surface *ab* upon orientation of mica and stilpnomelane is very slight (see Plate III, Figs. 15, 18). Maxima K and H are present in all four diagrams and coincide almost exactly, thus pointing to the existence of a pair of *s*-surfaces intersecting at about 80° as indicated by the full lines in the inset circle of Plate III, Fig. 18. Two prominent submaxima D and E developed in the diagram for stilpnomelane are each also present in one or other of the two

[9] In the quartzose layers cracks approximately parallel to *ac* are conspicuous in this section.

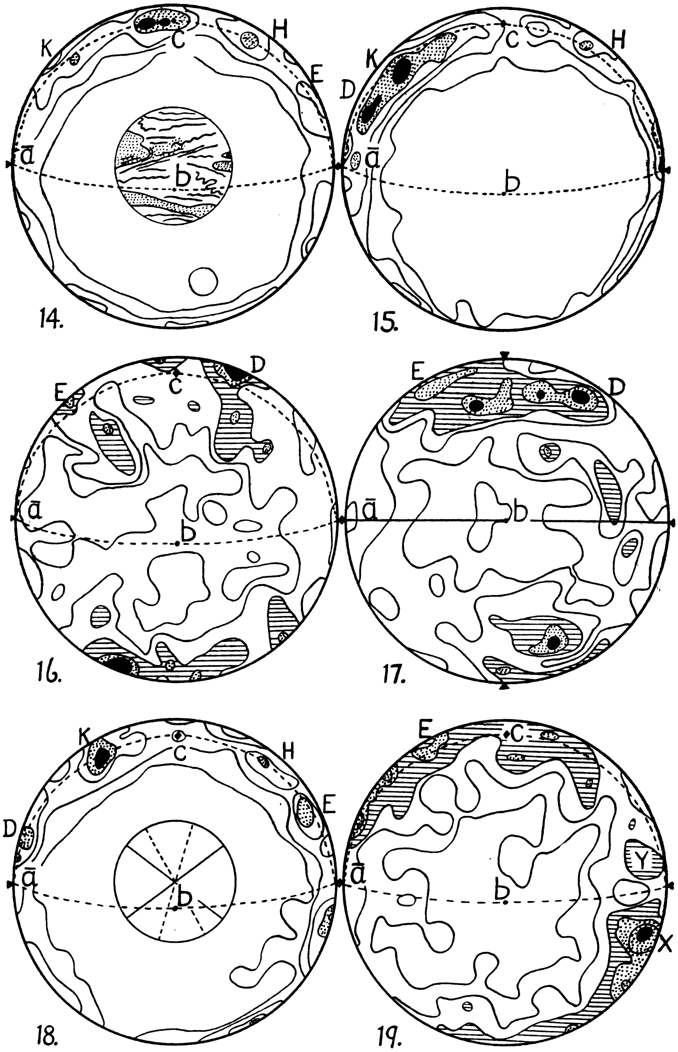

PLATE III.

Fig. 14. No. 4722, Muscovite, 300 flakes in albite-mica layers; rotated 180° about *a*. Contours 8, 6, 4, 2, 0.3%. Diameter of inset circle, 20 mm.; stippled portions are vein-like quartzose layers.

Fig. 15. No. 4722, Muscovite, 200 flakes in quartzose layers; rotated 180° about *a*. Contours 8, 6, 4, 2, 0.5%; maximum concentration, 10%.

Fig. 16. No. 4722, Quartz, 330 grains in quartz-rich layers; rotated 180° about *a*. Contours 4, 3, 2, 1, 0.3%.

Fig. 17. No. 4722, Quartz, 250 grains in quartz-rich layers, measured in section parallel to *bc* and rotated 90° about *c*. Contours 4, 3, 2, 1, 0.4%.

Fig. 18. No. 4722, Stilpnomelane, 150 flakes in quartzose layer; rotated 180° about *a*. Contours 8, 6, 4, 2, 0.7%. Positions of *s*-surfaces corresponding to K and H (full lines) and to D and E (broken lines) are shown in inset circle.

Fig. 19. No. 4713, Quartz, 400 grains in veins A_1, A_2; rotated 180° about *a*. Contours 5, 4, 3, 2, 1, 0.25%.

mica diagrams for the same rock, and are believed to express the influence of late movements accompanying the phase of deformation which was responsible for the development of the main maxima (similarly lettered) in the quartz fabric.

Specimen No. 4713

Locality: Entrance to Outram Glen, West Taieri, 200 yds. N of bridge across Taieri River.

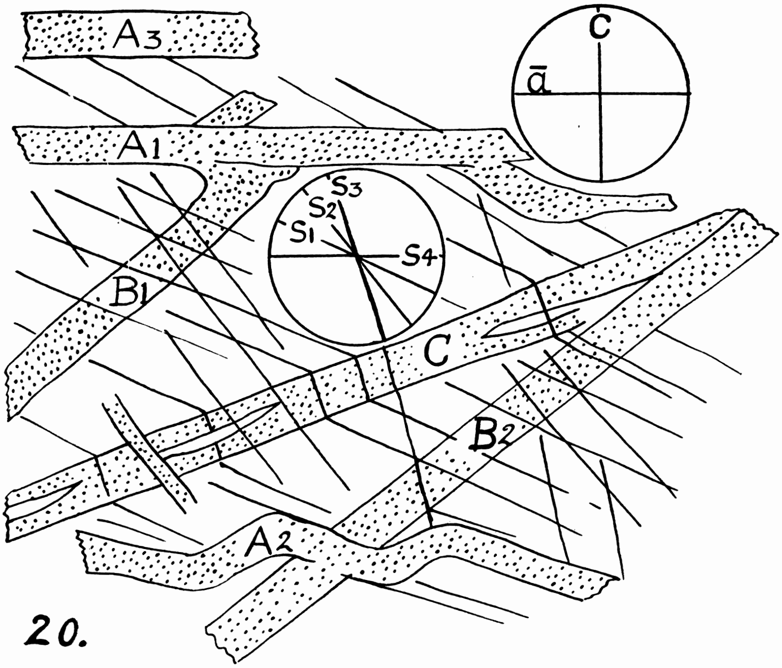

20.

Fig. 20. No. 4713, diagrammatic representation of structures visible in the field of a thin section cut perpendicularly to *b*. Dotted areas are veinlets of quartz; lines parallel to S_1, S_2, and S_3 indicate trends of strings of mica.

Schistosity (*ab*) rather imperfect, strike 70°, dip 7° to S.
Lineation *b* strong, strike 160°.
Joints vertical, strike 70° and (in a few cases) 160°.
Thin section cut at 82° to *b*.

In sections cut transversely to *b*, veinlets of quartz 1 mm. to 3 mm. wide, containing but small amounts of albite chlorite and muscovite, cut in several directions across the albite-mica-chlorite matrix in which yet other structural trends are visible. The structures observed within the field of a thin section, shown diagrammatically in Fig. 20, may be summarized thus:

The most conspicuous veins of quartz conform to three principal trends making angles of zero (A), 40° (B) and 20° (C) respectively with the megascopic schistosity (S_4). Veins of type A are clearly of somewhat later origin than those of type B which they cut in two places, while the vein C is probably the earliest of all since it appears to have been cut by B_2 in the manner indicated in Fig. 20. However, examination of the hand-specimen and of sections cut parallel to *ab* and *bc* respectively show that all three types of vein intersect in *b*, and have therefore formed parallel to (h0l) surfaces of the fabric. Development of all three types of vein therefore dates from the main stage of metamorphism in which the lineation developed parallel to *b*.

The most prominent banding (S_1) in the matrix lies at 15°-25° to the schistosity and is crossed locally by two others, S_2 and S_3, making angles with the schistosity of 50° and 70° respectively. These two latter are perhaps the result of local variation in trend of a single set of *s*-planes, but the mica and chlorite diagrams favour the existence of two distinct sets as just recorded. The schistosity itself (S_4) is inconspicuous in the thin section but its influence becomes apparent in fabric diagrams for mica and chlorite occurring in the matrix. In several places lines of chlorite and mica parallel to S_1 pass without change of direction through veins of types A and B, but where they cut C they are deflected so as to lie parallel to S_3. No such deflection of S_2 was noted in the section examined.

The lineation *b* is parallel to the line in which the various S-planes S_1-S_4 intersect. Hair cracks perpendicular to the schistosity but making angles of 75° with *b* are abundantly developed in the quartz veins as seen in the *ab* and *bc* sections; their geographic strike is 55° E of N.

Quartz diagrams were prepared separately for veins A_1 (250 grains), A_2 (150 grains), A_1 plus A_2 (400 grains, Plate III, Fig. 19), B_1 (225 grains, Plate IV, Fig. 21), B_2 (225 grains, Plate IV, Fig. 22) and C (250 grains, Plate IV, Fig. 23). These are markedly similar in the characteristic girdle slightly eccentric as to *b*, the positions of maxima D, E, X, and Y, and the strong minimum cutting the girdle in the top right and bottom left quadrants. The following table shows the positions of the maxima in the quartz diagrams in comparison with the trends of S_1 S_3 and S_4 as observed in the thin section. Both are measured clockwise from the point

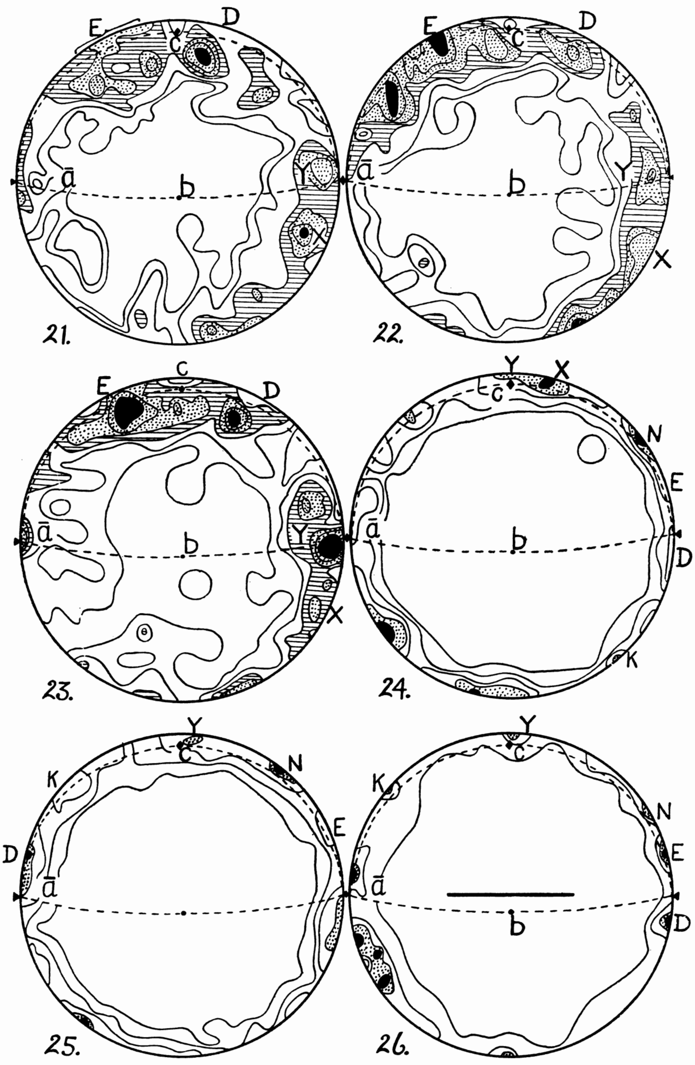

Plate IV

Fig. 21. No. 4713, Quartz, 225 grains in vein B_1; rotated through 180° about *a*. Contours 5, 4, 3, 2, 1, 0.5%; maximum concentration, 6%.

Fig. 22. No. 4713, Quartz, 225 grains in vein B_2; rotated through 180° about *a*. Contours 5, 4, 3, 2, 1, 0.5%.

Fig. 23. No. 4713, Quartz, 250 grains in vein C; rotated through 180° about *a*. Contours 5, 4, 3, 2, 1, 0.4%; maximum concentration, 6%.

Fig. 24. No. 4713, Muscovite, 170 flakes in matrix; rotated through 180° about *a*. Contours 8, 6, 4, 2, 0.6%.

Fig. 25. No. 4713, Chlorite, 200 flakes in matrix (measured on same traverses as mica for Fig. 24); rotated through 180° about *a*. Contours 8, 6, 4, 2, 0.5%.

Fig. 26. No. 4713, Chlorite, 77 flakes in vein A_1; rotated through 180° about *a*. Contours 8, 6, 4, 1.3%.

where the *a* axis cuts the boundary of the projection. The strongest maxima are in italics.

Maximum	Fig. 19	21	22	23	Trace of Visible S
X	*20°*	*20°*	*30-35°*	25°	S_1 15-25°
E	65	50– 75	*65*	*65*	S_3 70
D		*100–105*	120	*115*	
Y	170	175	180	*185*	S_4 180

Close correspondence between X, E and Y, and S_1, S_3 and S_4 respectively is strong evidence supporting development of the maxima in question by preferred orientation of quartz grains with their optic axes parallel to the three *s*-planes. The fourth maximum D has no apparent connection with any visible structure, but from its analogous position with that of the maximum D present in quartz diagrams for all other rocks described above it is interpreted as evidence of an invisible set of slip-planes inclined at a mean angle of 70° to the schistosity (as measured anticlockwise from *a*). Growth of quartz crystals at right angles to the vein walls has probably had a negligible influence on the present quartz fabric. In diagrams for veins A_1, A_2, and B_1 none of the maxima corresponds to a concentration of axes normal to the vein walls, while, although the maxima at E in vein C (Plate IV, Fig. 23) and at X in vein B_2 (Plate IV, Fig. 22) could conceivably be the result of growth orientation, the presence of similarly situated maxima in diagrams for other veins could not so be explained.

The possibility that the quartz is oriented with a rhombohedral or the basal plane is one or more set of visible *s*-surfaces has not been overlooked. This is considered improbable but is difficult to eliminate with certainty. Neither of the maxima X nor Y could be so related to any of the *s*-surfaces observed in the thin section, but D could conceivably represent a concentration of grains with (0001) parallel to S_1, or alternatively D and E together could constitute a ring maximum related to S_4. However, in many diagrams for other rocks (e.g. Plate I, Fig. 2, Plate II, Fig. 10, Plate III, Figs. 16, 17, Plate V, Fig. 31, Plate VII, Figs. 39, 40) maxima resembling D and E of the present diagrams occupy similar positions with reference to the geographic horizontal plane, regardless of the trend of the schistosity or other visible *s*-surfaces in the rocks in question. The possibility of control of orientation of the quartz by gliding on a rhombohedral or the basal plane is remote in such cases. In most of these other diagrams moreover, D and

E are so sharply separated that they cannot be regarded as together constituting a single ring maximum. The interpretation of the quartz fabric of No. 4713 given in the preceding paragraphs has thus been made with due regard to the fabric data obtained from other rocks in this field. More direct evidence of the actual existence of the invisible *s*-planes assumed to account for maximum D in the quartz diagrams is afforded by the appearance of an appropriately situated submaximum in several of the mica diagrams (e.g. Plate IV, Figs. 24, 25, 26).

The relative intensities of the different quartz maxima vary considerably when Plate III, Fig. 19, Plate IV, Figs. 21, 22, and 23 are compared. This condition might be explained on the one hand by differences in age and hence in tectonic history of the various veins, or on the other by differences in trend and in relative position of veins with reference to one and the same movement plan. The latter alternative is much the more probable, since the presence of the same maxima in all four diagrams points to operation of the same sets of *s*-planes in all three types of vein, while differences between diagrams for veins of different types (e.g. A_1 and B_1) are no more marked than for veins of the same type (e.g. B_1 and B_2). Strings of mica and chlorite parallel to S_1 continue across vein C as streaks alined parallel to S_3 and then reassume their S_1 trend after leaving the vein (cf. Fig. 20). The change in direction of slip so indicated is not a simple refraction of a set of *s*-planes at a mechanically significant surface, such as is generally familiar in rocks where slaty cleavage cuts alternating arenaceous and argillaceous bands. In the rock now under consideration movement on S_3 has affected the fabric of all parts of the rock and has been followed by later slip on S_1; where the S_1 slip-surfaces impinged upon veins (type C) of a particular orientation in relation to the movement plan, the movement was apparently taken up and continued across the vein by slip on the previously established surfaces S_3. This sequence of events deduced from the structure observed in the thin section (cf. Fig. 20) is substantiated by the weakness of submaximum X and prominence of E in the quartz diagram for vein C (Plate IV, Fig. 23).

Differential movement subparallel to the megascopic schistosity S_4 as indicated by maximum Y is least marked in veins A which themselves trend parallel to S_4, though even here a slight influence of S_4 as an active slip-surface is shown by slight but definite concentration at Y (Plate III, Fig. 19)

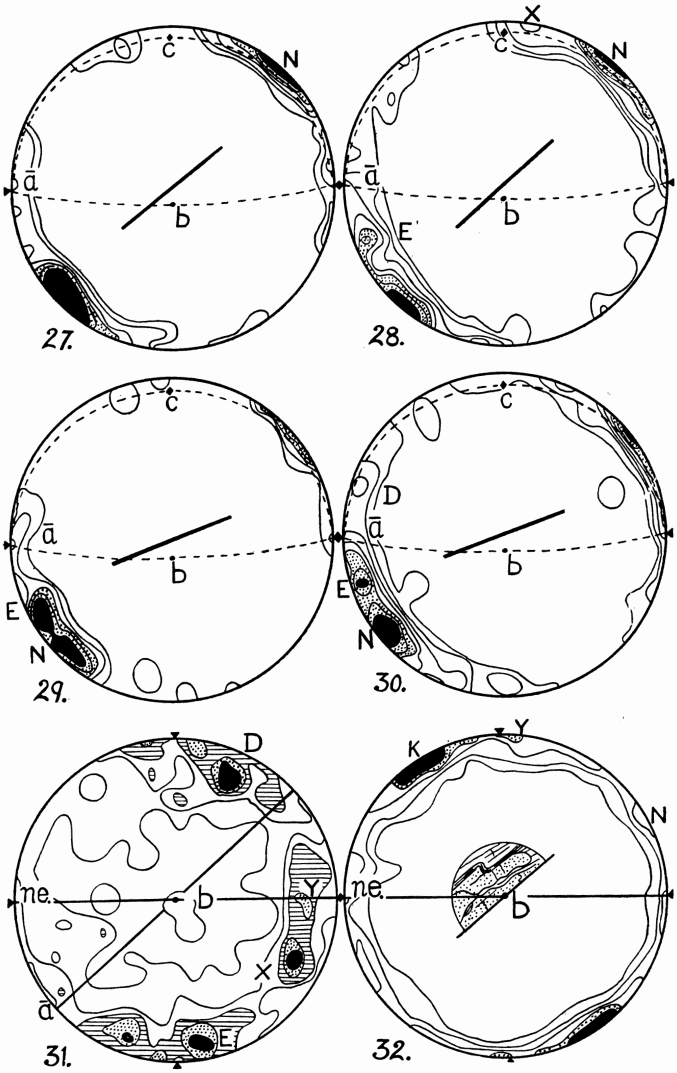

PLATE V.

Fig. 27. No. 4713, Muscovite, 55 flakes in vein B_2; rotated through 180° about *a*. Contours 12, 10, 8, 6, 4, 2%; maximum concentration, 20%.

Fig. 28. No. 4713, Chlorite, 100 flakes in vein B_2; rotated through 180° about *a*. Contours 12, 10, 8, 6, 4, 2, 1%; maximum concentration, 15%.

Fig. 29. No. 4713, Muscovite, 33 flakes in vein C; rotated through 180° about *a*. Contours 15, 12, 9, 6, 3%; maximum concentration, 20%.

Fig. 30. No. 4713, Chlorite, 150 flakes in vein C; rotated through 180° about *a*. Contours 12, 10, 8, 6, 4, 2, 0.7%; maximum concentration, 15%.

Fig. 31. No. 4697, Quartz, 350 grains; rotated through 180° about horizontal diameter. Contours 4, 3, 2, 1, 0.3%; maximum concentration, 5%.

Fig. 32. No. 4697, Muscovite, 200 flakes; rotated through 180° about horizontal diameter. Contours 8, 6, 4, 2, 0.5%; maximum concentration 12%. Structure of thin section is indicated in inset circle (quartzose areas stippled).

separated from maximum X by a minimal area. The submaximum between X and E in Plate III, Fig. 19 is found on comparing partial diagrams for veins A_1 and A_2 to be confined to the latter, and is therefore interpreted as due to local oscillation of S_1 in vein A_2, probably connected with the undulating course of the latter (cf. Fig. 20).

Small undeformed flakelets of chlorite and mica are present in equal quantities in the matrix of the rock, but in the veins chlorite is more plentiful than mica. The fabrics for the two minerals as determined for different parts of the section are closely similar though not identical. General diagrams based upon measurements in four representative traverses across the albite-mica-chlorite matrix were prepared for muscovite (170 flakes, Plate IV, Fig. 24) and chlorite (200 flakes, Plate IV, Fig. 25). Diagrams have also been drawn to show the preferred orientation of both minerals in veins of all three types: for muscovite, Plate V, Fig. 27 (55 flakes in vein B_2) and Plate V, Fig. 29 (33 flakes in vein C); for chlorite, Plate IV, Fig. 26 (77 flakes in vein A_1), Plate V, Fig. 28 (100 flakes in vein B_2) and Plate V, Fig. 30 (150 flakes in vein C). In all these the maxima and submaxima coincide with the poles of the various observed *s*-planes for the section as a whole, or with poles of planes corresponding to vein B or the quartz maximum D. In the following table their angular positions as measured clockwise from the *a* fabric axis are summarized, high and moderate intensity being indicated respectively by bold face and italic figures in question. (See footnote 7.)

Slight eccentricity of the mica and chlorite girdles with reference to *b* may be observed in most of the diagrams, just as for the rocks already described.

	Matrix		Vein A_1	Vein B_2		Vein C			
Maximum	Fig. 24 Mica	Fig. 25 Chlorite	Fig. 26 Chlorite	Fig. 27 Mica	Fig. 28 Chlorite	Fig. 29 Mica	Fig. 30 Chlorite	Figs. 21-23 Quartz	Poles of Surfaces
D	10°	**15°**	**10°**					280°-300°	
K	*50°*	45°	40°						B 50°
Y	*90°*	*95°*	*90°*						S_4 90°
X	**105°**				100°				S_1 105°-115°
N	**145°**	**130°**	**145°**	**135°**	**130°-135°**	**135°**	**140°**		S_2 140°
E	165°	155°	**160°**		*160°*	**160°**	**160°**		S_3 160°

The full sequence of events during deformation of the rock cannot be reconstructed from the data recorded in the fabric diagrams for quartz, mica, and chlorite, but the following points

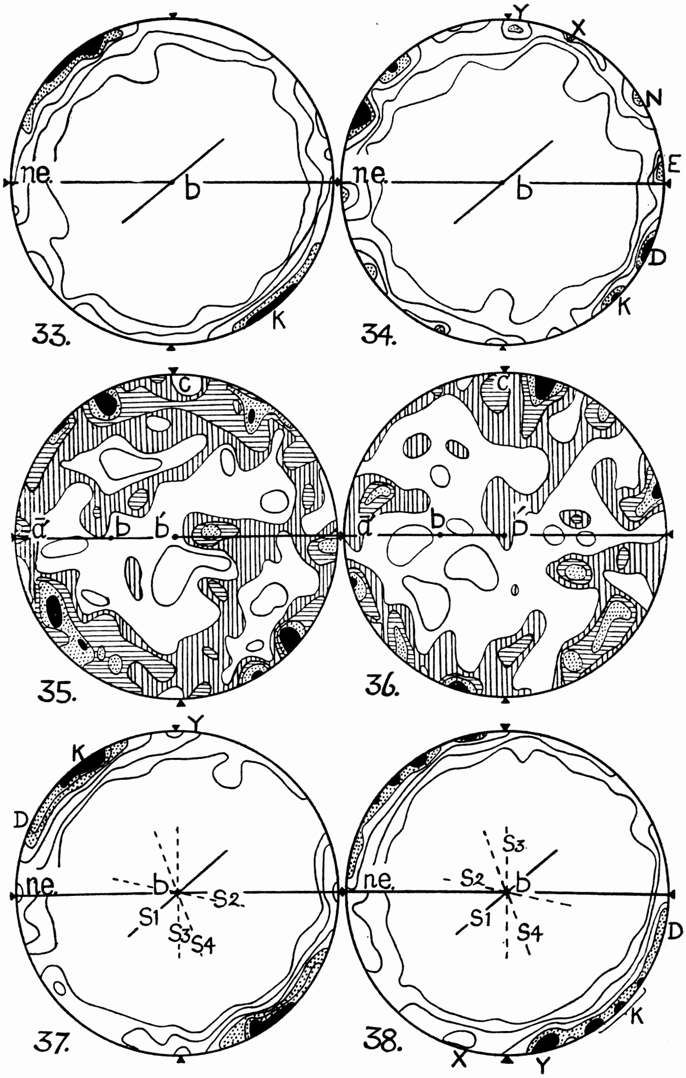

Plate VI.

Fig. 33. No. 4697, Chlorite, 200 small flakes in quartzose areas; rotated through 180° about horizontal diameter. Contours 8, 6, 4, 2, 0.5%; maximum concentration, 10%.

Fig. 34. No. 4697, Chlorite, 150 coarse flakes in chloritic aggregates; rotated through 180° about horizontal diameter. Contours 8, 6, 4, 2, 0.7%; maximum concentration, 10%.

Fig. 35. No. 4711 (Section 1), Quartz, 350 grains in lensoid aggregates; rotated through 180° about *a'*. Contours 2.5, 2, 1.5, 1, 0.3%; maximum concentration, 3.5%.

Fig. 36. No. 4711 (Section 2), Quartz, 380 grains in lensoid aggregates; rotated through 180° about *a'*. Contours 2.5, 2, 1.5, 1, 0.3%; maximum concentration, 3%.

Fig. 37. No. 4708, Muscovite, 200 flakes in thin micaceous streaks parallel to S_1; rotated through 180° about horizontal diameter. Contours 10, 8, 6, 4, 2, 0.5%; maximum concentration, 15%.

Fig. 38. No. 4708, Muscovite, 250 minute flakes in quartz-albite; rotated through 180° about horizontal diameter. Contours 8, 6, 4, 2, 0.5%; maximum concentration, 9%.

may be established and serve to indicate that deformation must have been a long-continued and complex process:

(1) Since all sets of visible *s*-planes and veins intersect in *b*, these structures almost certainly must have originated during a major period of deformation in which the tectonic axis *b* main-

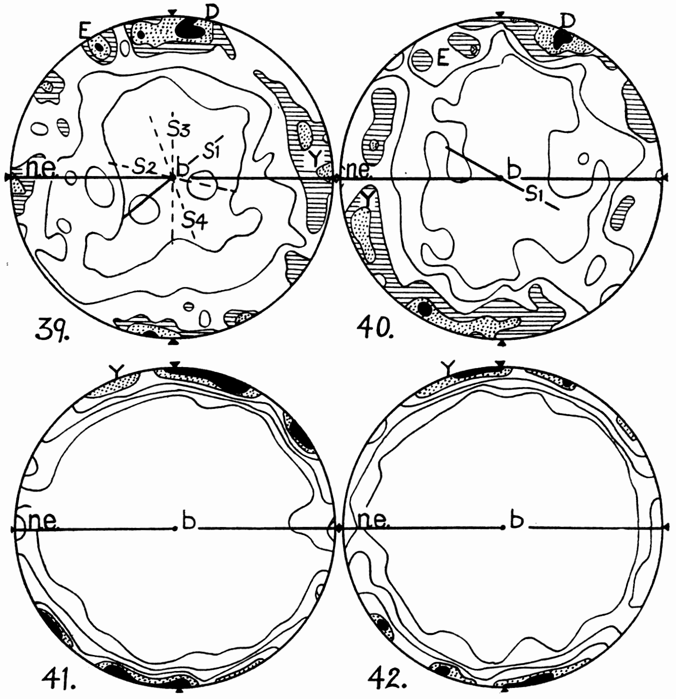

PLATE VII.

Fig. 39. No. 4708, Quartz, 400 grains; rotated through 180° about horizontal diameter. Contours 4, 3, 2, 1, 0.25%; maximum concentration, 4.5%.

Fig. 40. No. 4709, Quartz, 400 grains; rotated through 180° about horizontal diameter. Contours 4, 3, 2, 1, 0.25%; maximum concentration, 4.5%.

Fig. 41. No. 4709, Muscovite, 250 flakes in micaceous bands; rotated through 180° about horizontal diameter. Contours 8, 6, 4, 2, 0.4%; maximum concentration, 10%.

Fig. 42. No. 4709, Muscovite, 250 flakes in quartzose layers; rotated through 180° about horizontal diameter. Contours 8, 6, 4, 2, 0.4%; maximum concentration, 9%.

tained a constant trend of 160°. It is unlikely that the six sets of surfaces involved (S_1, S_2, S_3, and A, B, and C) could have been initiated simultaneously, and indeed we have already noted that the veins appear to have developed in the order C, B, A. It is not improbable that each of these latter may represent a set of (h0l) surfaces corresponding to a complementary set of principal (h0l) slip-planes (S_2, S_1, S_3) during

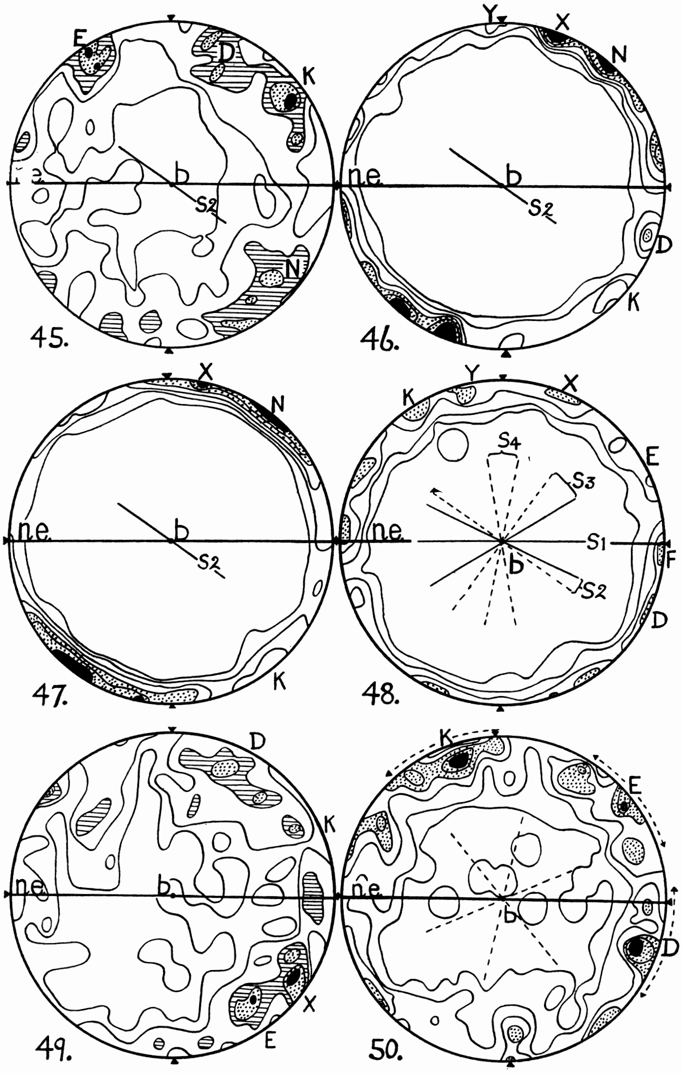

PLATE VIII.

Fig. 45. No. 4707, Quartz, 350 grains. Contours 4, 3, 2, 1, 0.3%.

Fig. 46. No. 4707, Muscovite, 150 flakes in quartzose areas. Contours 10, 8, 6, 4, 2, 0.7%; maximum concentration, 12%.

Fig. 47. No. 4707, Muscovite, 300 flakes in micaceous layers. Contours 10, 8, 6, 4, 2, 0.3%; maximum concentration, 12%.

Fig. 48. No. 4702, Muscovite, 200 flakes. Contours 6, 4, 2, 0.5%; maximum concentration, 7%. *s*-planes visible in measured specimen indicated by full lines; *s*-planes visible only in Nos. 4704, 4705 (adjacent specimens) indicated by broken lines.

successive phases of the deformation, for the angular interval A-C-B is approximately the same as S_3-S_2-S_1. The secretion of quartz veinlets during this earliest and most important stage of deformation would render the rock less homogeneous for reaction to later deforming forces.

(2) The youngest veins, those of type A, show the influence of movements on every type of slip-plane recorded in the rock, if diagrams for quartz and chlorite are compared. It is obvious then that in the later phases of deformation movement was by no means confined to newly initiated sets of surfaces but occurred also on those developed during the earliest stages. Furthermore, owing to the inhomogeneity already noted in the mass undergoing deformation, change of direction of slip at surfaces of physical discontinuity, such as veinwalls, appears to have been frequent. Thus movement on S_1 in the matrix was continued along S_3 in the vein C as shown both in Fig. 20 and in the corresponding quartz diagram (Plate IV, Fig. 23).

(3) Comparison of corresponding chlorite and mica diagrams shows that for any measured part of the section the orientation patterns of these two minerals are almost identical; e.g. in vein C (Plate V, Figs. 29, 30) there are strong maxima at E and N, while in diagrams representing muscovite and chlorite in the micaceous matrix (Plate IV, Figs. 24, 25) N is strong, E very weak, and other maxima, Y, K, and D are developed sympathetically to varying degrees.

(4) On the other hand there is no apparent relation between the relative intensities of the quartz maxima on the one hand and those for mica or chlorite in the same part of the section on the other. For example, the chlorite fabric of vein A (Plate IV, Fig. 26) is no more closely related to the quartz fabric of vein A (Plate III, Fig. 19) than to that of veins B (Plate IV, Figs. 21, 22) or C (Plate IV, Fig. 23). A striking difference that persists for diagrams representing all parts of the section is the strong influence of S_2 (maximum N) on the mica and chlorite fabrics contrasted with the absence of any such effect in quartz diagrams. These differences are interpreted as resulting from late imprint of the main features of the quartz fabric after the mica and chlorite had attained

---

Fig. 49. No. 4702, Quartz, 250 grains. Contours 4, 3, 2, 1, 0.4%.

Fig. 50. No. 4702, Calcite, 200 grains. Contours 5, 4, 3, 2, 1, 0.5%. Dotted lines at centre indicate directions of deduced slip-surfaces corresponding to the three ring maxima at D, E, and K. Dotted arcs subtend angles of 40°.

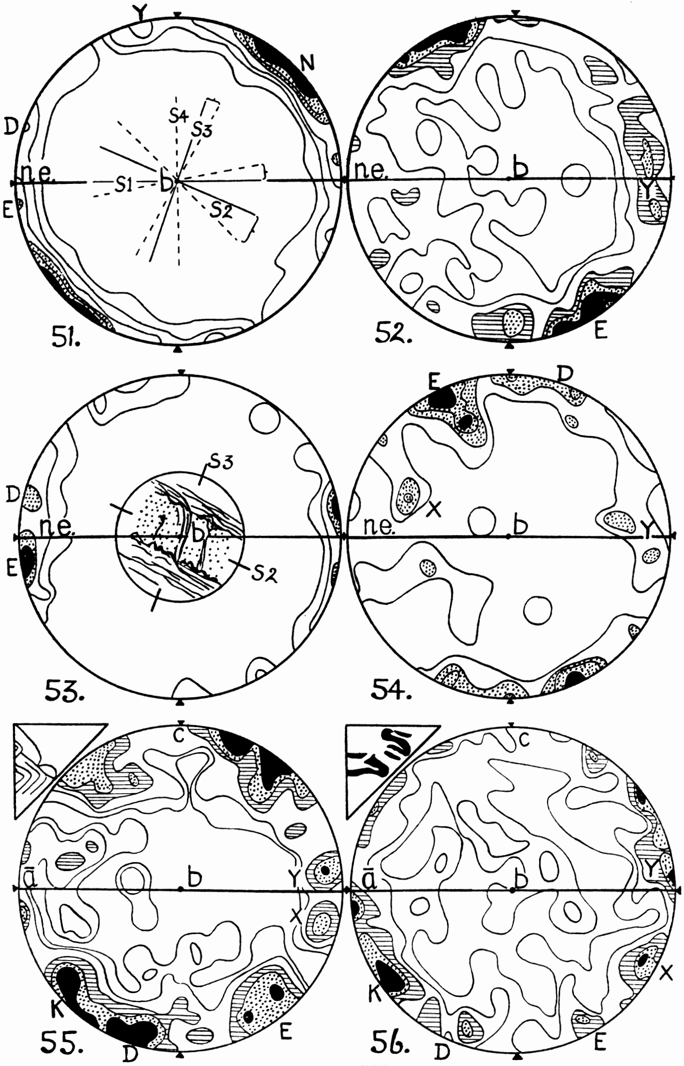

PLATE IX.

Fig. 51. No. 4703, Muscovite, 300 flakes; rotated through 180° about horizontal diameter. Contours 10, 8, 6, 4, 2, 0.3%. Full lines at centre indicate *s*-surfaces for No. 4703; broken lines *s*-surfaces for No. 4706.

Fig. 52. No. 4703, Quartz, 400 grains; rotated through 180° about horizontal diameter. Contours 4, 3, 2, 1, 1.25%; maximum concentration, 5%.

Fig. 53. No. 4703, Muscovite, 50 flakes in bands parallel to S_3 cutting quartzose layer; rotated 180° about horizontal diameter. Contours 14, 10, 6, 2%.

Fig. 54. No. 4703, Quartz, 80 grains in fine-grained band parallel to S_3 cutting coarser quartzose layer; rotated 180° about horizontal diameter. Contours, 7, 5, 3, 1%.

approximately their present orientation. These latest movements must have taken place for the most part in such of the initial *s*-planes as were favourably situated for the new movement plan, but the eccentricity of the quartz girdles shows that the directions of late movement with the old S_1, S_3, etc., were perpendicular to a new tectonic axis slightly oblique to *b*, with which the transverse hair-cracks visible in *ab* and *bc* sections may also be correlated. It is noteworthy that the various quartz diagrams for No. 4713 show the influence of not only the steeply inclined *s*-planes deduced in the case of other rocks described above, but also *s*-planes of low inclination, viz. S_1 (maximum X) and S_4 (maximum Y).

Steeply Dipping Schist From Deep Stream.

Specimen No. 4697

Locality: Deep Stream, 300 yds. below bridge on main Outram-Middlemarch Road.

Schistosity (*ab*) well developed, strike 150°, dip NE at 40°.

Lineations: *b*, strongly defined, 150°;
b′, fine and discontinuous, 165°-170°.

Joints widely spaced, vertical, strike 60°-65°.

A polished end-section of the hand-specimen cut at right angles to *b* shows a dark laminated micaceous matrix studded with irregular quartzose pencils a few millimetres in thickness that appear to have originated by buckling, rupture, and rotation of originally continuous laminae. The matrix has been drawn around and between the pencils to give rise to a well developed but somewhat undulose schistosity. Similar features are shown by all three specimens (Nos. 4697-4699) collected from this vicinity.

In thin section the light-coloured pencils are seen to consist of quartz and albite in equal quantities, with chlorite as a minor constituent. The fabric diagram for quartz is based on measurements of 350 grains, all within the same pencil. When plotted, as in Plate V, Fig. 31, with the geographic horizontal as horizontal diameter of the projection there is a strong resemblance to quartz diagrams for rocks of the Outram-Mt. Hyde traverse (e.g. Plate III, Fig. 17, Plate IV, Fig. 21, etc.),

---

Fig. 55. No. 4715, Quartz, 213 grains in area A of Fig. 57. Contours 4, 3, 2, 1, 0.5%; maximum concentration, 6%. Structure of measured area is shown in top left corner.

Fig. 56. No. 4715, Quartz, 250 grains in folded quartzose layers adjacent to B and C, Fig. 57. Contours 4, 3, 2, 1, 0.4%; maximum concentration, 5%. Outline of measured area is shown in black in top left corner.

but this similarity no longer holds if Plate V, Fig. 31 is rotated through 40° so as to superpose *ab* in the diagrams in question. This is clear evidence that the quartz fabric, with its characteristic eccentric girdle and its maxima grouped around *c*, the pole of the horizontal plane, was impressed upon the rock after the inclined schistosity had developed. This is to be distinguished from other instances to be described later in which the quartz fabric, originally imprinted upon rocks with horizontal schistosity, had subsequently been tilted without distortion, in local movements of yet later date. It should be noted that this is a diagram in which D and E might have been interpreted as constituting a single ring maximum; but even on this interpretation, the corresponding slip-plane in the fabric would be quite unrelated to *ab*, the only well developed visible *s*-surface.

The mica diagram, Plate V, Fig. 32, represents 200 flakes measured in the micaceous streaks along six traverses across the schistosity. The girdle, slightly eccentric as to *b*, is dominated by a maximum K corresponding to the megascopic schistosity, but there are also a distinct submaximum Y, which may be correlated with Y of the quartz diagram, and a faint submaximum N representing a transverse *s*-structure that may also be detected by inspection of the thin section.

Chlorite is of two kinds, occurring respectively as small isolated flakes in the quartz-albite pencils (Plate VI, Fig. 33, 200 flakes), and as aggregates of coarse, thick plates apparently of late origin and localized at boundaries of quartzose and micaceous areas (Plate VI, Fig. 34, 150 flakes). The outstanding feature of Plate VI, Fig. 33 is the maximum K representing flakes lying with (001) parallel to *ab*, but in Plate VI, Fig. 34 the girdle pattern is more strongly developed and in addition to maximum K there are distinct and sometimes strong concentrations at D, E, X, and Y, all corresponding to similarly lettered maxima in the quartz diagram, and at N, which is correlated with the transverse *s*-structure mentioned in connection with Plate V, Fig. 32. This is a striking instance of the way in which the coarse chlorite crystallizing at a late stage, though itself undeformed, is strongly influenced by all observed *s*-structures, including those which governed preferred orientation of the quartz.

UNIVERSITY OF OTAGO,
DUNEDIN, NEW ZEALAND.

To be continued.